Arch. Mech., 35, 1, pp. 37–62, Warszawa 1983

Characteristics of stress-strain behaviour associated with thermoelastic martensitic transformation

N. NAKANISHI (KOBE)

IN THE PRESENT paper, first, the nature of martensitic transformation, especially its thermoelastic characters, for example, the mobility of interface and twin boundaries, typical crystal structures and their mutability under the applied stress, have been briefly reviewed. Secondly, so-called "pseudoelastic" stress-strain behaviour has been presented in connection with "superelastic", "ferroelastic" and "shape memory" phenomena. In these typical stress-strain curves the close relation between the shapes of stress-strain curves and the change in morphological and crystal structures has been discussed.

W pracy omówiono przede wszystkim naturę przemiany martenzytycznej, a zwłaszcza jej charakterystykę termosprężystą, np. ruchliwość powierzchni międzyfazowych i bliźniaków, typowe struktury krystaliczne i ich zmienność pod przyłożonym obciążeniem. Ponadto przedstawiono tzw. "pseudosprężystą" zależność między naprężeniem i odkształceniem w związku ze zjawiskami "supersprężystości", "ferrosprężystości i "pamięci kształtu". Na przykładzie typowych krzywych "naprężenie-odkształcenie" omówiono bliskie związki między kształtem tych krzywych a zmianą struktur morfologicznych i krystalicznych.

В работе обсуждена прежде всего природа мартенситного превращения, а особенно ее термоупругая характеристика, например, подвижность межфазных поверхностей и двойников, типичные кристаллические структуры и их переменность под приложенной нагрузкой. Кроме этого представлена т. наз. „псевдоупругая" зависимость между напряжением и деформацией в связи с явлениями „суперупругости", „ферроупругости" и „памяти формы". На примере типичных кривых „напряжение-даформация" обсуждены близкие связи между формой этих кривых и изменением морфологических и кристаллических структур.

1. Martensitic transformation

1.1. Nature of martensitic transformation

THE MARTENSITIC transformation, the name of which has arisen from the quenched-in structure of steels, belongs to the first-order phase transition and the volume change associated with the martensitic transformation requires a few percents. Usually in this transition, an atomic shear operates cooperatively in the specific direction on the close-packed plane and, accordingly, each atomic displacement amounts to considerable percents of lattice distance. The martensitic transformation, therefore, has a character of diffusionless-type in the crystal lattice in which the atom-vacancy interchange does not occur. However, this transformation occasionally requires a small atomic displacement associated with the shear movement. This is called "atomic shuffling" [1].

Moreover, the martensitic transformation has so far been recognized in terms of the following characteristics: (i) The interfaces between the parent phase and the martensite

phase remain undistorted and unrotated during the transformation and we call these habit planes. (ii) There exists a specific orientation relationship between their crystal lattices. (iii) Recent studies report that premonitory phenomena have been found in the temperature range above the transition temperature [2].

As the martensitic transformation is not associated with a composition change, the free-energy curves of both parent and martensite phases, as a function of temperature, may be represented as shown schematically in Fig. 1, where T_0 represents the thermodynamic equilibrium temperature between the two phases; that is, $\Delta F^{M\to P}$ (at T_0) $= F^P - F^M = 0$. $\Delta F^{M\to P}$ (at M_s) $= F^P - F^M$ represents the driving force required for the nucleation

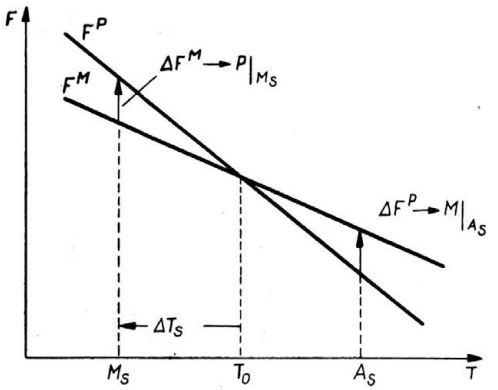

FIG. 1. A schematic free energy-temperature relation between martensite and parent phases.

of the martensite which arises from the involvement of nonchemical energies such as surface and strain energies in the nucleation process. Usually T_0 is approximated by the equation $T_0 = (M_s + A_s)$. For example, a fairly large value of the driving force, $\Delta F_{M_s}^{M\to P} = 1255.5$ J/mol (Fig. 1), has been reported in Fe–C alloys, meaning that the nonchemical energy change associated with the martensitic transformation cannot be explained by using only the elastic energy term in an iron-based alloy system. Thus the free-energy change associated with a growing martensite can be expressed as [3] $\Delta F = v \cdot \Delta g_{ch} + v \cdot \Delta g_{el} + S \cdot \sigma + K \cdot \delta$. Here v represents a volume transformed, Δg_{ch} and Δg_{el} are respectively the chemical free-energy change and the elastic energy change, and σ and δ are the surface energy and the work necessary for plastic deformation, respectively. The last term $K \cdot \delta$ represents a characteristic of the ferrous-martensite, the energy of which must be irreversibly dissipated during the martensitic transformation.

1.2. Thermoelastic martensitic transformation

As seen in Table 1, there exist some metals and alloys with ferrous and nonferrous groups, where the groups A, B and C represent some typical martensitic alloys with different characters: (i) Difference in temperature hysteresis $(A_s - M_s)$: We can see a fairly large hysteresis ~400 K in an F_e — 30 at% Ni alloy (Group A), while with group B the

Table 1. Classification of various martensitic alloys according to the magnitude of lattice softening.

Group A no lattice mechanical instability	Group B moderate lattice mechanical instability	Group C drastic lattice mechanical instability
Fe–C	Cu–, Ag–, Au– and Ni–	In–X alloys
Fe–Cr–Ni	β Hume-Rothery phases	(X = Tl, Cd, Hg ...)
Fe–Mn–C	U.	A15 compounds (V_3Si, Nb_3Sn)
Co	Fe–Ni (Ni% > 30%)	
Co–Ni	Fe–Pt (near Fe_3Pt)	antiferromagnetic alloys
Fe–Ni (Ni% < 30%)		(Mn–Cu, Mn–Ni, ...)

hysteresis, $(A_s - M_s) \cong 15$ K, is seen to be very small in an Au — 47.5 at% Cd alloy (Fig. 2). (ii) Significant difference in the manner of reversible transformation: In the groups B and C, transformation proceeds by continuous growth of the martensite on cooling. If cooling is stopped, growth ceases, but if it is resumed, the transformation proceeds by further growth of the martensite until impingement with grain boundaries or other martensite plates occur. Now, if heat is applied, the reverse transformation occurs by the backwards movement of the interface, thus annihilating the shape strain originated

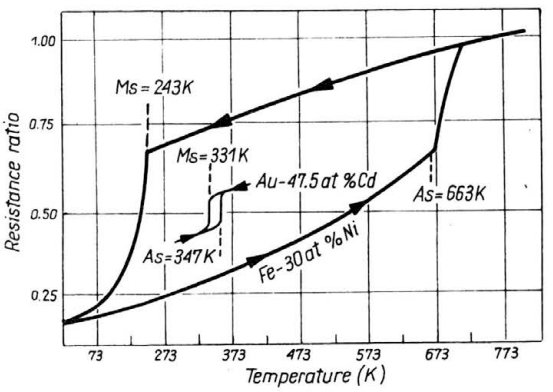

FIG. 2. Difference in trensformation temperature hysteresis A_s–M_s between Fe–Ni and Au–Cd alloys.

during the cooling transformation, without leaving any relief, and the martensite crystals, revert completely to the original orientation. On the other hand, for the group A, once a martensite plate grows to a certain size upon cooling, it does not grow any more by further cooling, because the interface evidently becomes immobile at this stage. Thus the reverse transformation does not occur by the backwards movement of the interfaces but rather by nucleation of the parent phase within the martensite plates. We call the groups *B* and *C* "thermoelastic martensite".

In the thermoelastic martensitic transformation, the last term $K \cdot \delta$ is not so important, even negligible, but the terms $v \cdot \Delta g_{el}$ and $S \cdot \sigma$ appear to be very important. When a martensite plate grows up to a certain size upon cooling, the growth can be stopped by the thermoelastic balance (between two terms Δg_{ch} and Δg_{el}). In the case of iron-alloys,

where a fairly large driving force is required, this thermoelastic balance cannot be satisfied and, consequently, plastic deformation occurs. It was reported in Fe–Ni alloys [4] that several hundreds of martensite plates can be formed within 10^{-6} seconds. Figure 3 shows a growing martensite plate which has {121}-type internal twins. The transformation such as shown above, which is characterized by a mobile interface and a small driving force, is called "thermoelastic martensitic transformation". This interface reversibility is closely connected with the crystallographical reversibility. The elastic movement of

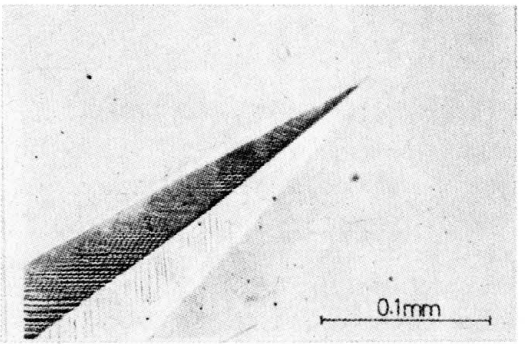

FIG. 3. A growing martensite plate (Cu–Al–Ni).

interface boundaries associated with a temperature change or applied stress may be realized only when a martensite crystal is coherently connected to the surrounding matrix crystal and this coherency is maintained during the whole process of the growth or shrinkage. In order to examine the interface structure, a scanning electron microscopy was recently carried out with γ_1' martensite subjected to the single interface transformation [5]. Even though constraints from the surrounding matrix are absent in this type of transformation, {121} γ_1' internal twins were observable in the γ_1' martensite, manifesting that the twins are necessary in order to make the interface an invariant plane, as is assumed in the phenomenological theory. The width of the twins were different from one specimen to the other, but they extended right up to the interface under an optical microscope. The density of twins are usually higher just behind the interface than in the interior of the martensites, as seen from Fig. 4a [5] and as suggested for the In–Tl alloy [6]. This is because the reduction of elastic energy by thinning of twins becomes more important near the interface. Although the interface is usually straight under an optical microscope, some deviations are observed under the scanning electron microscope. The internal twins are usually tapered toward the interface and pointed there, as seen in Fig. 4b. It was also sometimes observed that twins are projected into the matrix as if they were independent variants of the martensite. These observations indicate that, although the elastic energy at the interface can macroscopically be minimized at the interface by the introduction of twins, as is shown in Fig. 4c, the local stress concentration or the stress due to coherency is always present at the interface. This local stress concentration probably makes the interface very mobile, as is actually observed.

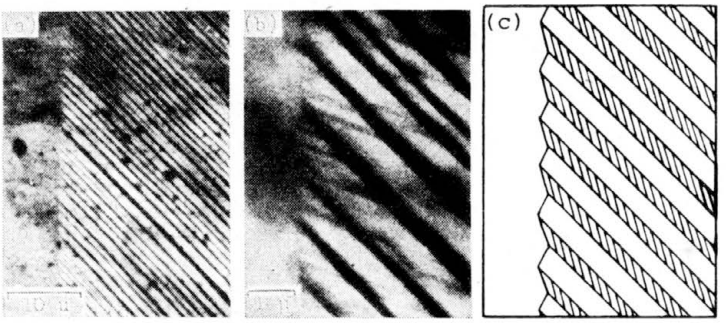

FIG. 4. Scanning electron micrographs of a thermoelastic interface between β_1 matrix and γ_1' martensite, and a schematic interface expected from the phenomenological theory [5].

1.3. Characteristics of the crystal structures observed in thermoelastic martensites

So far, a number of thermoelastic martensitic alloys have been found; these are, TiNi, AuCd, AgCd, AuAgCd, CuZn, CuAlNi, CuAlZn, CuSn, NiAl, InTl and Fe_3Pt [7]. Here we can recognize a common crystallographic relation among the long period stacking order structures, which are usually transformed from ordered β_1 phases, except for In–Tl (fcc $\rightleftharpoons$ fct) and Fe_3Pt (fcc $\rightleftharpoons$ bct ?).

As shown in Fig. 5, the crystal structures of the transformation products are of the close-packed layer structure, such as fcc and hcp-like. It is assumed that the close-packed layer is transformed from a {110} bcc plane, that is, the transformation shear plane. For the shear direction there are two possibilities, $\pm$ [110], on each plane. If shear takes place in the same direction on every plane parallel to (110), the resulting structure is fcc-like (Fig. 5e).

If alternate shear on every other plane takes place, the resulting structure is hcp-like (Fig. 5b). If plus and minus shears occur periodically, the existence of resulting struc-

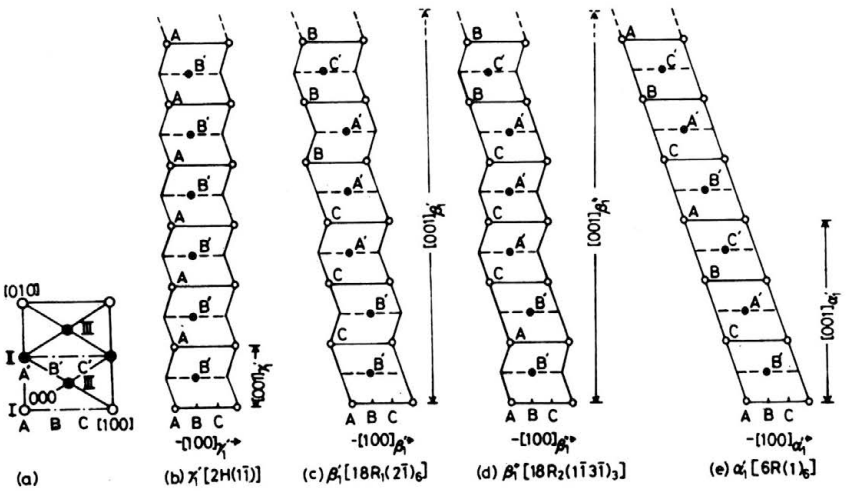

FIG. 5. Crystal structures of various stress induced martensites. a) Atomic arrangement and possible stacking sites in the common basel plane. b–e) Stacking sequence of each structure, viewed from $[010]_\gamma$ = $= [010]_{\beta''}$ directions [8].

tures can be possible, when energetically favourable. For example, β_1' [$18R_1(2\bar{1})6$] and β_1'' [$18R_2(\bar{1}\bar{1}3\bar{1})_3$] structures (Fig. 5c and d) often appeared in thermally-formed and stress-induced martensites of Cu–Al–Ni alloys [8], where the Arabic numeral, 18, indicates the number of layers in one period and the letter, R_1 or R_2, following it stands for rhombohedral symmetry.

In many cases these close-packed structures have superlattices. The superlattices are considered to be formed because the product phases in the martensitic transformation inherit the atomic ordering of the parent phases. Most β phases in noble metal based alloys have the Fe_3Al-type ($D0_3$) superlattice or CsCl-type (B2) superlattice. All of these superlattices are denoted by β_1. In the Fe_3Al-type structure two kinds of atomic planes, A_1 and B_1, parallel to $(110)_{bcc}$ are alternately stacked, as shown in Fig. 6. It is then considered that the martensite structures resulting from shears on these $(110)_{bcc}$ planes consist of six kinds of close-packed layers that are shifted relative to each other in the direction

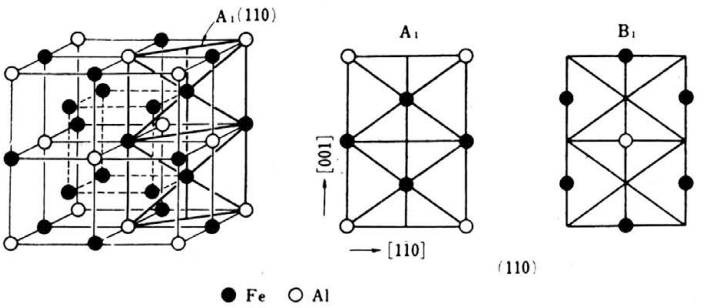

FIG. 6. Fe_3Al-type crystal structure: A_1 and B_1 are two kinds of atomic planes which are parallel to $(110)_{bcc}$.

parallel to the close-packed plane. For example, the 2H(hcp) structure has the $A\,B'$ stacking order, where the prime represents a change in the superlattice structure and the A', B' and C' planes are produced by shifting the A, B and C planes, respectively, as shown in Fig. 7.

In the case of the $9R$ structure, such as Cu–Zn martensite [9], the nine layers $ABCBCACAB$ are taken as the unit cell, the symmetry is then orthorhombic. While in the case of the 18R structure, the eighteen layers $AB'CB'CA'CA'BA'BC'BC'AC'AB'$ are also taken because of the $D0_3$ ordered structure. Though the so-called long period stacking order structures have been commonly observed in many β phase alloys based on noble metals, another kind of martensite structure having different properties such as symmetry, morphologies, habit plane and lattice relationship between the parent and martensite phase, was studied by TADAKI *et al.* [10]. Analysis was carried out by means of electron microscopy and electron diffraction. They reported that all the electron diffraction patterns taken from Au-50 at % Cd martensite are well explained by the trigonal lattice model recently proposed from X-ray diffraction studies.

Two martensite variants are in a mirror relation to each other with respect to the {100} plane of the β_1 matrix and the habit plane is approximately parallel to that plane. The orientation relationship between the trigonal martensite and cubic matrix is obtained as

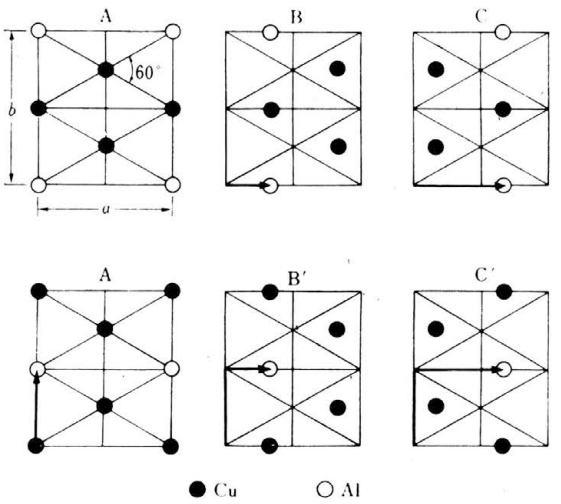

FIG. 7. Atomic arrangement in six kinds of close-packed layers in Cu_3Al martensite.

follows: $(001)_{tri}//(111)_{\beta 1}$, $[1\bar{1}0]_{tri}//[10\bar{1}]_{\beta 1}$ or $[100]_{tri}//[11\bar{2}]_{\beta 1}$. It is of interest to note that the trigonal martensite does not undergo intrinsically the so-called lattice invariant shear.

Figure 8 shows a typical transmission electron micrograph of β_1' martensite obtained in a Cu-23.7 at% Al alloy [11], and streaks in the [001] direction in electron diffraction patterns indicate that there are a number of errors in atomic shuffling, where the β_1' martensite is thought to be produced from the β_1 structure by shear accompanied by shuffling of the atomic planes. In the photo, several martensite plates are seen in the layer struc-

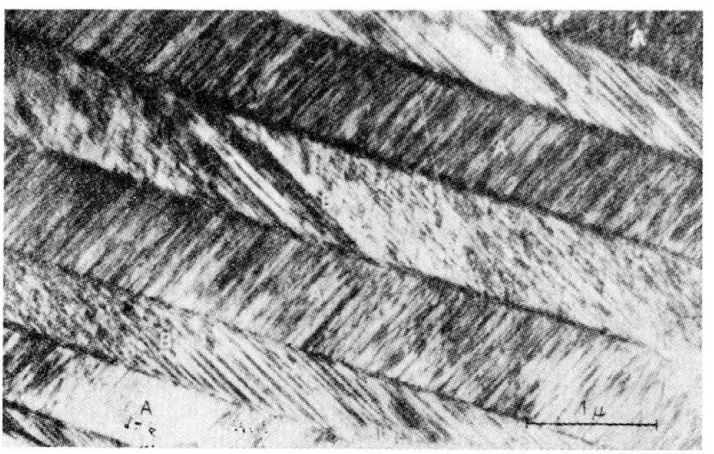

FIG. 8. Electron micrograph of a β_1' martensite in Cu–23.7 at % Al alloy; each plate has many stacking faults [11].

ture and striations tending in the same direction are observed in every other plate. The direction of the streaks seen in the electron diffraction pattern is perpendicular to the (001) plane. Therefore, the striations are due to stacking faults on the (001) plane.

On the other hand, the γ_1' martensite observed in Cu–Al and Cu–Al–Ni alloys [9] has a 2H type stacking layer structure and transformation twins are seen in γ_1'. The twinning plane of the transformation twins is {201} or {121} in orthorhombic coordinates and {1101} in hexagonal coordinates.

2. Pseudoelastic mechanical behaviour and shape memory phenomena

Recently, pseudoelasticity associating with martensitic transformations of noble-metal based alloys of the β-brass type has been investigated with great interest [12]. The alloys are characteristically soft and flexible, like rubber, in comparison with martensites of ferrous alloys with great hardness. When the martensites of noble-metal based alloys are deformed and thereafter heated above the transition temperatures (A_f), the deformation is removed, thus the original shape is recovered (i.e. the shape memory effect). This interesting behaviour is strongly related to mechanisms of martensitic transformation and is, therefore, a suitable subject of investigation of the nature of martensitic transformation. Described in brief below is the pseudoelastic behaviour in stress-strain curves which were recently measured.

Here the term "pseudoelasticity" involves the following stress-strain behaviour; (i) "superelaticity" (and or rubber-like behaviour ([1])), which means a phenomenon in that in a stress-strain relation, relatively large strains, attained on loading beyond the elastic limit, recover completely on unloading at a constant temperature, (ii) "ferroelasticity" [13] and (iii) as will be discussed below, stress-strain curves obtained in the case where large strains, attained on loading beyond the elastic limit, recover partially on unloading and the superelasticity is not complete.

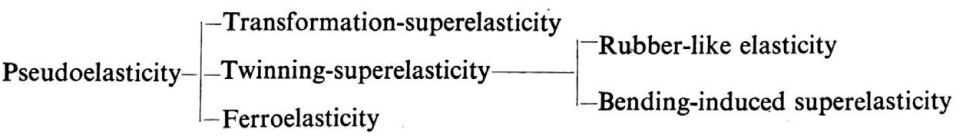

2.1. Rubber-like elasticity

Linear and cross-linking polymers show, in general, rubber-like elasticity and the Young's modulus is of the order of 1 MPa which is considerably smaller than that of

([1]) According to OTSUKA and WAYMAN [12], "pseudoelasticity" means two cases: superelasticity and the rubber-like effect. These authors used the terminology "superelasticity" if the stress-strain behaviour is caused by a stress-induced martensitic transformation and its subsequent reversion, and "rubber-like behaviour", which is generally indistinguishable from superelasticity on the basis of stress-strain curves alone, if the behaviour is characteristic solely of the martensitic phase and does not involve a phase transformation.

solids, ~1 GPa. The moduls is linear to the absolute temperature, and deformation by an external stress is attributed to a change in entropy. For example, as shown in Fig. 9 [14], the stress-strain curve of a polymer shows that even a deformation far beyond the yield value may vanish with the relief of applied stress. The stress-strain curve does not follow Hooke's law and is inelastic. Here the superelasticity is realised because while strain is not proportional to stress, it still vanishes when the stress is removed.

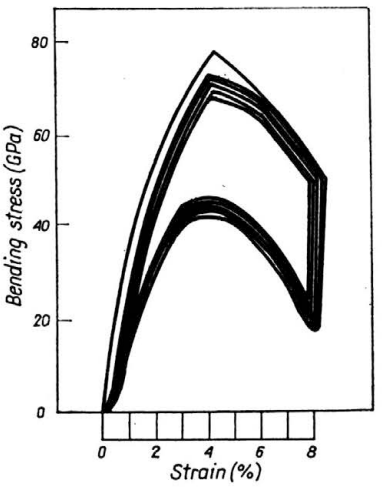

FIG. 9. Stress-strain curves in a polymer [14]).

2.1.1. Pseudoelastic stress-strain curve of Fe-Al ordered alloys. When a stress-strain curve of a single crystal with nearly Fe_3Al composition was obtained by tensile deformation, strain of a few percents remained and the superelasticity was not complete [15]. The following three conditions seem to be important for the superelastic behaviour: (i) Recovery of strain of ~15% is found only between Al 21 ~ 26 at% for the $\{110\}\langle 111\rangle_{b.c.c.}$ shear system and Al 23~29 at% for the $\{112\}\langle 111\rangle_{b.c.c.}$ system. (ii) Quenched alloys do not show superelasticity at all but do when annealed at temperatures where the ordered Fe_3Al lattice is stable. (iii) The superelasticity is not observed at 77 K but when alloys are heated to room temperature, the strain is recovered to ~90%. This is a shape memory-like behaviour, though any martensitic transition and or any reversible mobile twins are not found.

2.1.2. Stress-induced martensites (SIM) of Au-Cd alloys and superelasticity. When a single crystal of Au-47.5 at% Cd is under a tensile or compressive stress above A_f, such a double loop as shown in Fig. 10 is observed [12]. At point M in the figure, martensite is induced by stress and a sawtooth-like deformation is observed. When the stress is removed, the alloy is restored to the parent phase following a hysteresis loop. The different shape of the loops with tensile and compressive stresses comes from the different variants of the SIM's.

Many other martensitic alloys also show similar superelastic loops. Also some martensites below M_f show a similar behaviour. It seems, however, that there is no very clear-cut explanation of these complex phenomena. Experimental details will be described below.

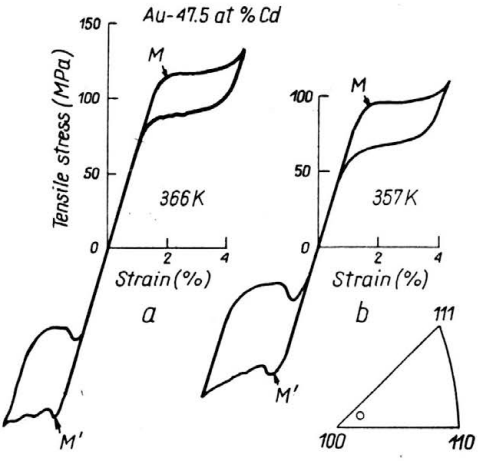

FIG. 10. Double hysteresis curves obtained by tension-compression test above M_s for Au–47.5 at % Cd.

2.2. Pseudoelasticity of thermoelastic martensites

2.2.1. Superelastic behaviour above A_f. Thermoelasticity means here that the growth of a thermal martensite is interfered by a balance between the thermal driving force and the elastic strain energy. Thermoelastic martensites show a reversible expansion and contraction depending on temperature, i.e. thermal elasticity.

A direct microscopic observation of the surface of Au-47.5 at% Cd-0.7 at% Cu single crystal under stress at 298 K ($\geqslant A_f$) was made [16] as shown in Fig. 11. When the yield point is approached, parallel bands appear at one end of the sample and grow toward the other end. When applied stress is reduced, the bands move on the other way around. Stripes appear only near the boundary between the martensite and the parent phase, and the martensite at some distance from the boundary is a single crystalline as shown directly by the X-ray Laue method. The martensite is orthorhombic with $a : b : c = 1 : 1.48 : 1.43$, and the orientational relation with the parent phase (CsCl-type) is $(011)_{CsCl} // (001)_{Orth}$, $[\bar{1}\bar{1}1]_{CsCl} // [\bar{1}\bar{1}0]_{Orth}$ in good agreement with that of the thermal martensite reported by CHANG and READ [17]. How SIM is formed depends on the relative orientation between the stress axis and the crystalline axes. For example, in Cu–Al–Ni alloys showing $\beta_1 \rightleftarrows \beta_1'$ transition [12], a needle-like martensite appears at various parts of the sample at the same time in the vicinity of the yield point of the stress-strain curve and grow to cover the whole sample volume. When a test is made at $M_s < T < A_f$, SIM is formed by the same mechanism but the strain is not completely recovered because of the remaining martensite below A_f.

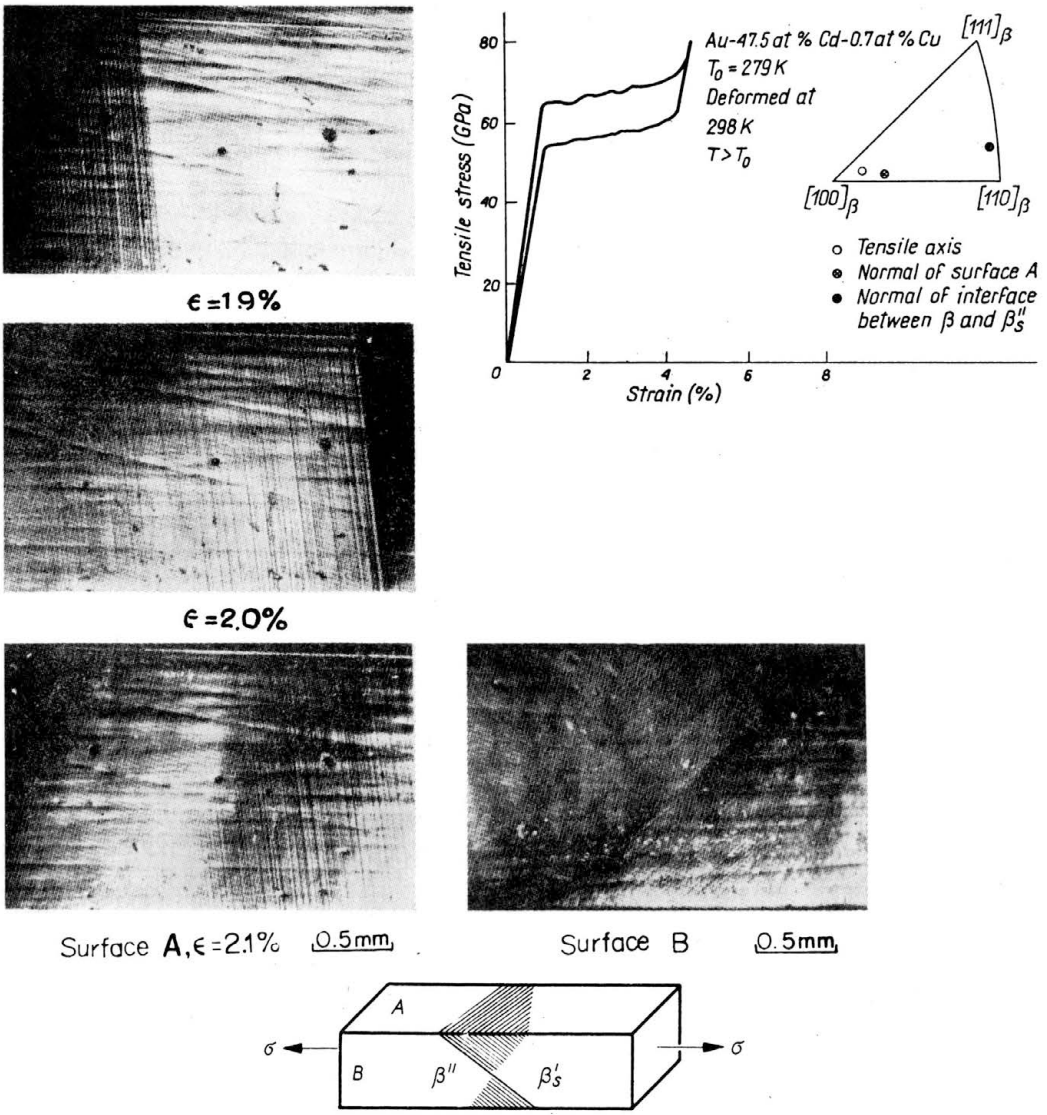

FIG. 11. Superelasticity and direct observation of the SIM formed in Au–47.5 at % Cd–0.7 at % Cu alloys at 298 K, i.e. above T_0.

In Fig. 12, (a–g) corresponds to the loading process, and (a'–g') corresponds to unloading. Upon loading, starting from the single crystal state in the β_1 matrix phase (a), no structural change occurs in the linear elastic range until point b is reached in the stress--strain curve, where a few martensite plates appear (lower right corner b). With increasing strain more and more plates are nucleated and some of them coalesce into thicker plates since only one variant is favoured by the Schmidt factor. Eventually at point e the specimen becomes essentially a single crystal, although a few plate-like matrix regions are still

observable. Thus the elongation between b and e ($\sim 7.2\%$) corresponds to that obtained from the shape strain of the stress-induced transformation. The further increase of stress to point f causes the specimen to become a complete single crystal of martensite. With further increase of stress no structural change is observable, and the curve between f and g is almost linear.

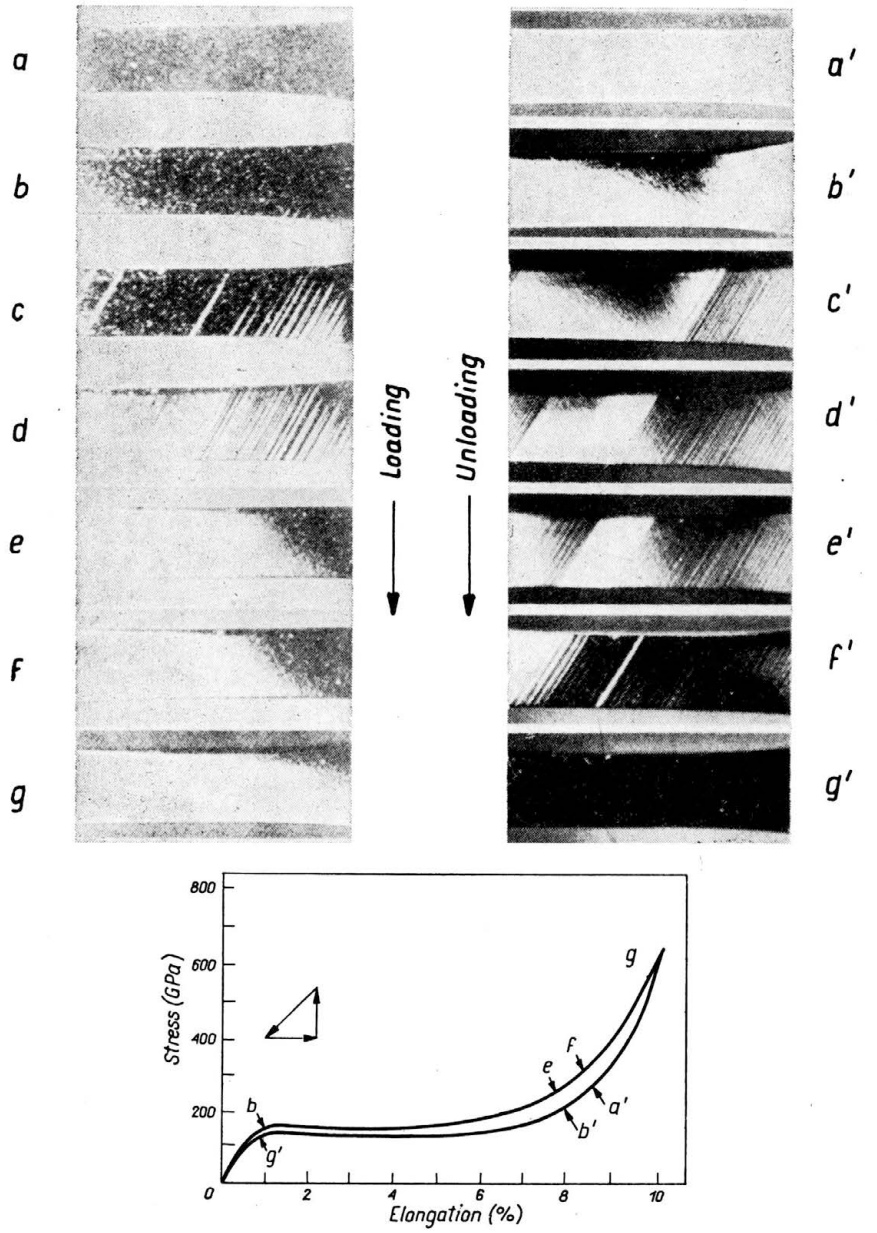

FIG. 12. Macroscopic morphological change associated with the $\beta_1 \rightleftharpoons \beta_1'$ transformation at 300 K [12].

In the above example the nucleation of martensite was uniform over the entire specimen, but in some specimens martensite formation was inhomogeneous and resembled Lüders band propagation. In these cases, the martensite was first nucleated nearly at the center of the specimen, and then with increasing strain several new martensite plates were nucleated in adjacent regions while coalescence occurred inside. Thus the transformation process was slightly different from specimen to specimen but the important point to be emphasized here is that the rate determining process is the nucleation of martensites in both cases, i.e. not the propagation of pre-existing plates. Upon unloading from point g no structural change occurs until point a' is reached, and at point b' thin plate matrix regions are nucleated in the martensite. With decreasing strains more and more matrix regions are nucleated, but the reverse transformation proceeds more or less like Lüders band propagation in contrast to the loading process. Eventually at point g' the specimen reverses to the original β_1 matrix.

2.2.2. Ferroelastic behaviour below M_f. Hysteresis loops on the stress-strain curve of the thermal martensite of Au-47.5 at% Cd subject to repeated tensile and compressive stresses is shown in Fig. 13. The loop for the first cycle is comparatively broad. The second and the following treatments result in quite the same loop, i.e. any work hardening is not observed. NAKANISHI *et al.* termed this elastic behaviour ferroelasticity [18] because it can be explained by analogy with the H–I curve of a ferromagnet and the E–P curve of a ferroelectric material. Indeed, boundaries between twins of independent martensites are shown to move reversibly depending on an external stress (tensile or compressive), and this is quite similar to, for example, the motion of magnetic domain walls by an external magnetic field. The ferroelastic behaviour is missing above A_f and the sample is restored to its original shape, i.e. the shape memory effect. Plastic strain obtained below M_s is not due to the slip and, therefore, is not permanent. The deformation strain is, in other words, recoverable on the occasion of the transformation of the martensite phase to the parent phase, and the original shape of the parent phase alloy is recovered.

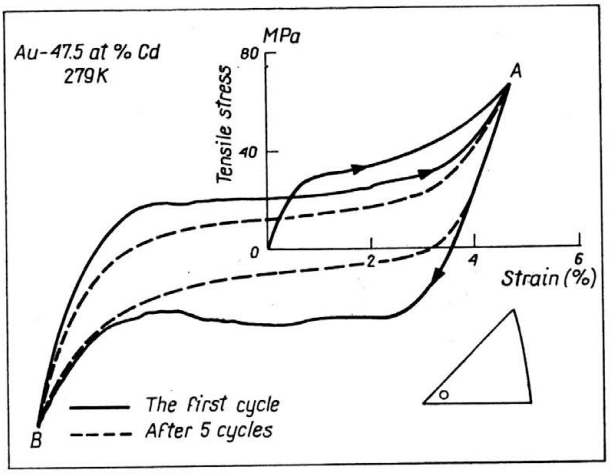

FIG. 13. Tension-compression hysteresis loops obtained below M_f for Au–47.5 at % Cd.

The self-accommodating character of the martensite: Optical microscopy has shown that the self-accommodating character is valid for the β-type martensite formation in the copper-base alloys and for some silver- and gold-based alloys. The β-type martensite is characterized by the formation of groups of martensite plates of four different variants; since differently oriented groups can be observed in one β-grain. A schematic diagram showing the spatial arrangement of the four martensite plate variants is given in Fig. 14a [20]. The figure shows the perspective top and front views of such a group. The mac-

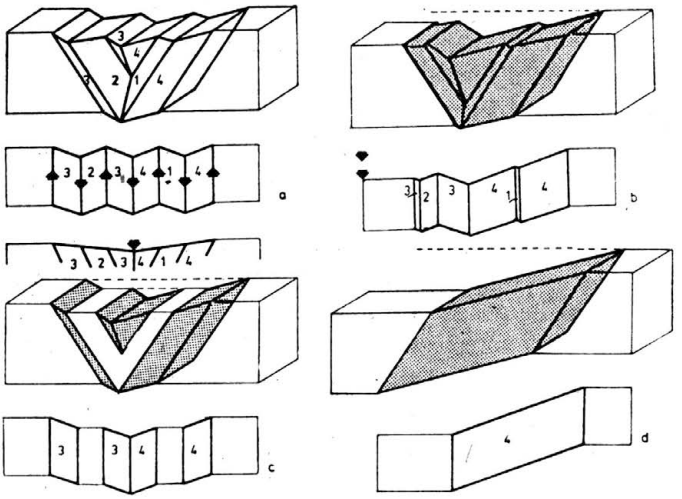

FIG. 14. Spatial arrangements of the four martensite plate variants.

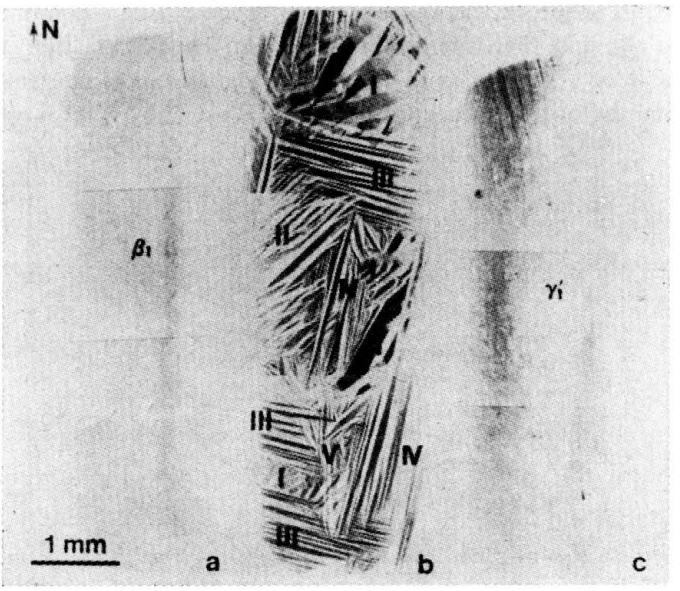

FIG. 15. Microstructural changes on cooling and stressing a specimen. a) Parent β_1 phase; b) Variants of γ_1' martensite produced on cooling; c) Single crystal of γ_1' martensite produced after tensile stressing the b) [21].

roscopic shape deformations of plates 1 and 4 and also of plates 2 and 3 are equal and roughly opposite; this is clearly visible in the top and front views. The macroscopic deformations of plates 1 and 2 and also of plates 3 and 4 are exactly equal and opposite. The formation of a group of nearly parallel martensite plates of variants 1 and 4 will result in a small shape deformation which is then compensated by changing over to the other pair of martensite plates of variants 2 and 3. We are thus dealing not only with the plane of minimum distortion (invariant plane strain) but also with the minimization of the three-dimensional volume distortion. If the sample is now slightly strained, the volume fractions of the four variants are not equal any more, meaning that the macroscopic deformation is not completely compensated (Fig. 14b). For this it is necessary that the martensite plate boundaries between the different variants be movable under the influence of stress. Such movement of the martensite plate boundaries has indeed been observed in earlier work [19]. A larger amount of macroscopic deformation can be obtained if only two martensite plate variants are formed instead of four (Fig. 14c). The maximum obtainable macroscopic deformation through stress-induced martensite formation is achieved by the formation of a single martensite plate variant (Fig. 14d).

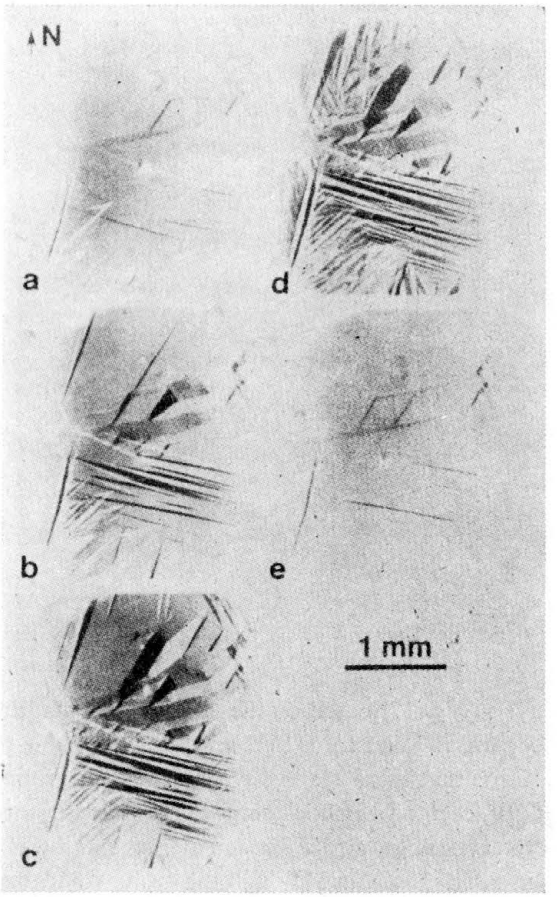

FIG. 16. Microstructural change on cooling and heating.

Self-accommodating transformation (zero macroscopic shape change on cooling and variant coalescence on stressing) in Ag-45 at % Cd: [21] Fig. 15a is an optical micrograph showing the surface of the entire gauge length of an unstressed tensile specimen at room temperature (β_1 phase). When this specimen was cooled below the M_s temperature, a self-accommodating thermoelastic martensitic transformation occurred, resulting in the distribution of habit plane variants, as shown in Fig. 15b below the M_f temperature. Further details concerning the thermoelastic and reversible nature of the transformation during cooling and heating are given in Fig. 16, where the region shown corresponds to the upper part of Fig. 15a. On cooling, the parent phase shown in Fig. 15a transforms thermoelastically, forming martensite plate groups (Fig. 16a–d), and on heating the plates reverse in an inverse manner (Fig. 16e) to the original parent phase.

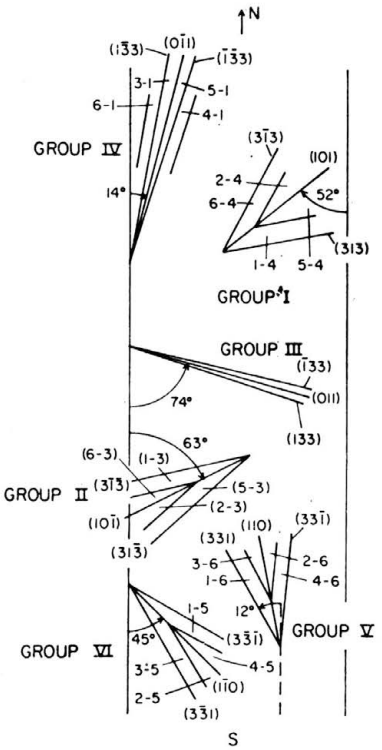

FIG. 17. Schematic representation of six types of martensite variant groups.

Stereographic analysis (Fig. 17) based on the observations that the boundaries between two variants in a shear are parallel to $\{110\}_\beta$ and that the habit planes of the variants are close to $\{331\}_{\beta_1}$ shows that there are five types of variant groups in Fig. 15b, namely groups I, II, III,IV and V, each of which is composed of four variants. The transformation twins in each plate of the variant group are extremely thin, and it was therefore not possible to contrast the twins in different colour although the twins could be detected as fine striations within the plates.

When the self-accommodating variant morphology shown in Fig. 15b was stressed in tension, variant coalescence occurred, and the entire gauge length region of the specimen eventually became a single crystal of martensite, except for regions near the grip ends of the specimens, Fig. 15c, upper. Similar observations were made on other specimens with the same orientation and on those with different orientations, and the final deformation product consisted of a single crystal of martensite. However, even though the end result is rather simple, the intermediate deformation processes can be somewhat complex, in that a different type of behaviour is generally observed for each variant group.

2.2.3. Superelasticity in Au-49.5 at% Cd alloy. In an Au-49.5 at % Cd alloy, since M_s is about 298 K, the thermal martensite β'', whose crystal structure has been determined as hexagonal or trigonal [22], was obtained at room temperature. In Fig. 18 the superelasticity of this alloy at 291 K is shown. A lamellar structure appeared just behind the moving interface during deformation, and a few millimeters behind the interface the lamellar

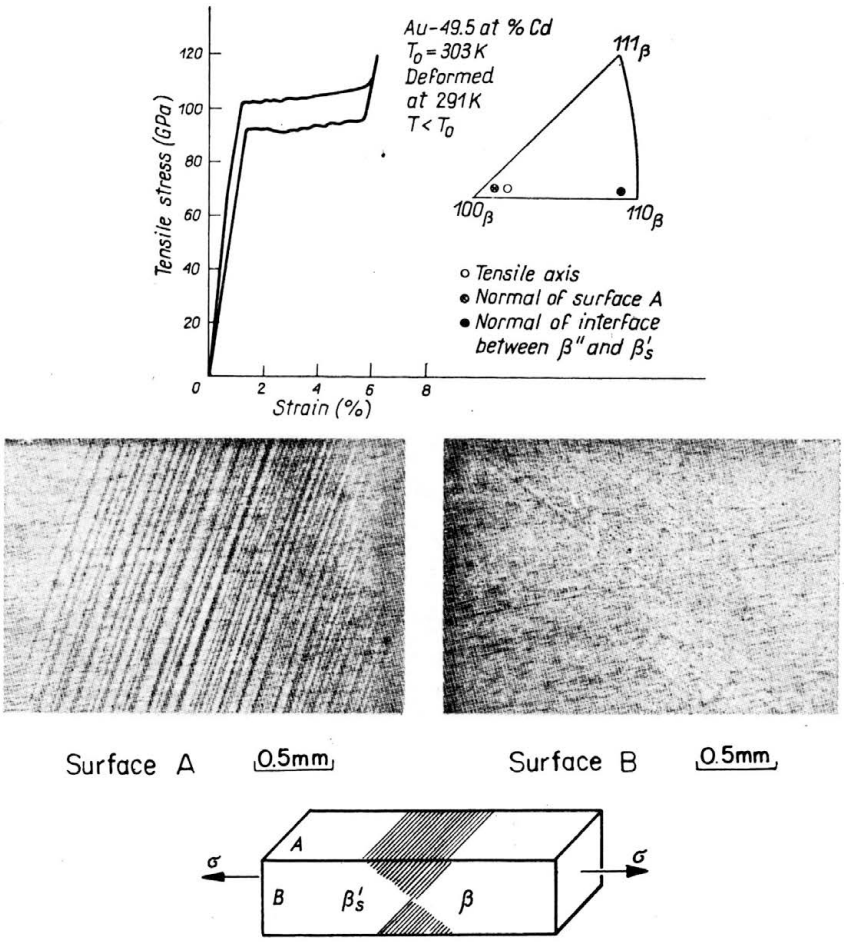

FIG. 18. Superelasticity and surface observation of the SIM in Au–49.5 at % Cd alloy at 293 K (i.e. below T_0).

merged into a single crystal of β_s' SIM (Stress-Induced Martensite). Upon unloading, the reverse motion of the interface was observed. However, the Laue-patterns show that this stress-strain curve is accompanied by a structural change from β'' to β_s', the same structure as that obtained in the SIM of Au-47.5 at % Cd-0.7 at % Cu alloy.

According to TADAKI *et al.* [10], the junction plane between two adjacent martensite variants is parallel to the $(1\bar{2}1)$ plane of the trigonal martensite, which corresponds to the {100} plane of the matrix, and the two martensite variants are in a mirror relation to each other with respect to that plane. The habit plane of the martensites is approximately parallel to the junction plane. The orientation relationship between the trigonal martensite and cubic martix is definitely obtained as follows: $(001)_M//(111)_\beta$, $[1\bar{1}0]_M//[10\bar{1}]_\beta$ or $[100]_M//[11\bar{2}]_\beta$, being nothing but the lattice correspondence between the two lattices previously adopted. The trigonal martensite does not undergo intrinsically the so-called lattice invariant shear, so that there exists no mobile twin boundary upon stressing. Therefore, it is understood that the ferroelastic loop cannot be obtained even below M_f upon applying stress in this alloy.

2.2.4. Superelastic (or rubber-like) behaviour of ageing below M_f. If a thermal martensite which shows a ferroelastic behaviour upon deformation is kept at room temperature and then examined, the stress-strain curve becomes superelastic and the critical stress increases with an increase in the keeping time. This phenomenon is observed in Au–Cd [23] and Au–Cu–Zn alloys [24]. For example, $Au_{26}Cu_{28}Zn_{46}$ with M_f = 305 K shows an almost superelastic behaviour if quenched to and kept at room temperature for 43200 sec. The ageing effect is missing above A_f, and when cooled to room temperature again the sample shows a ferroelastic rather than superelastic stress-strain curve, as shown in Fig. 19. It was found that $\varepsilon_2/\varepsilon_1$ increased with ageing time at 291 K below M_f temperature, where

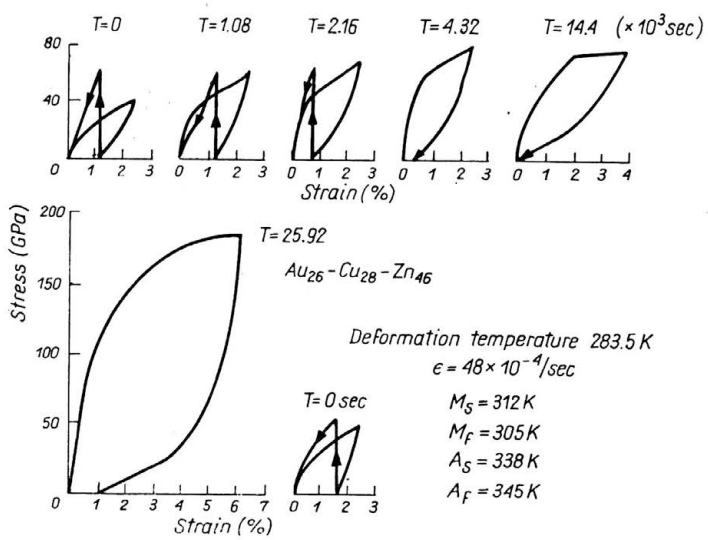

FIG. 19. Effects of ageing time on the stress-strain curves in Au_{26}—Cu_{28}—Zn_{46} martensite.

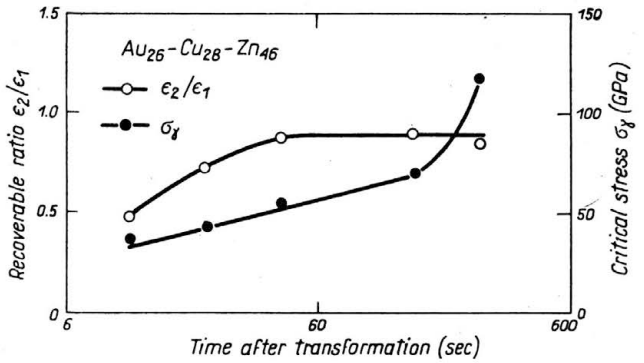

FIG. 20. Variation of the recoverable ratio, $\varepsilon_2/\varepsilon_1$, and the critical stress with time after transformation in Au_{26}—Cu_{28}—Zn_{46} martensite.

ε_1 was the total strain and ε_2 the strain recovered upon unloading the specimen. As shown in Fig. 20, the critical stress σ_γ increased with an increase in ageing time.

Figure 21 shows a superelastic loop in the first yielding stage of Au-47,5 at % Cd-0.3 at% Cu alloy which was aged at 293 K for one day after a thermal transformation. Without ageing after transformation, this first yielding stage exhibited a ferroelastic loop, i.e. residual strain existed. By direct observation of the electrolytically polished surface, it is seen in Fig. 21 that upon tensile loading after the ageing, one orientation of the twin

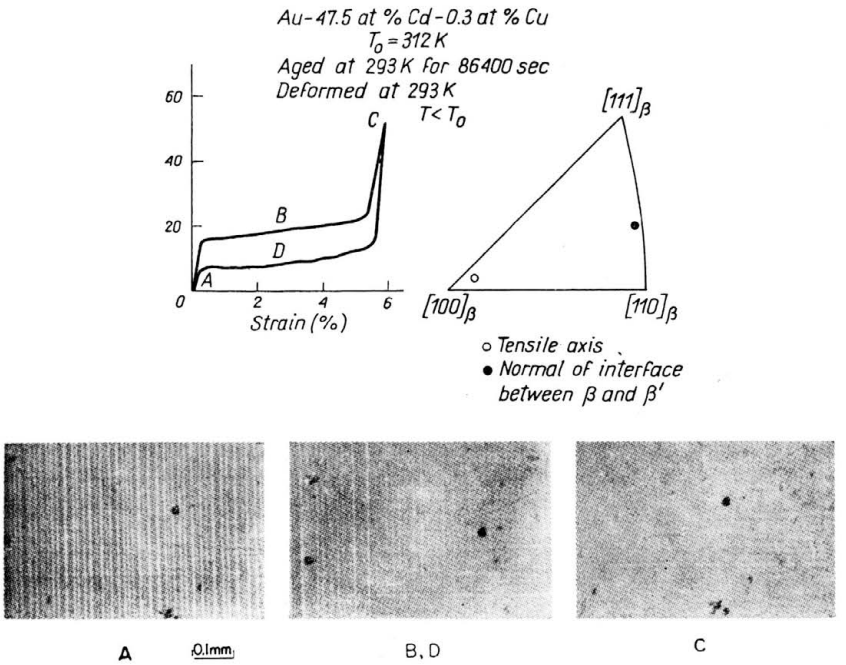

FIG. 21. Superelasticity and twin boundary motion in Au–47.5 at % Cd–0.3 at % Cu which was aged at 293 K for a day after the transformation. The normal to the habit plane of martensite is also shown.

relation grows at the expense of the other and finally a single oriented martensite is obtained ($A \rightarrow B \rightarrow C$); that upon unloading, these mobile twin boundaries, which have already been stabilized during the ageing, move back to the original positions ($C \rightarrow D \rightarrow A$), and a superelastic loop is obtained. This superelasticity is not related to the stress-induced martensitic transformation, but is considered to be associated with the reversible motion of the twin boundaries.

Concerning stabilization of twin boundaries by annealing, LIEBERMAN [25] proposed that shuffling of each atom becomes complete only after ageing so that boundaries can be mobile by a higher stress. In any case, an increase in the Young's modulus on ageing was found experimentally, indicating that a larger restoring force acts on the boundaries.

2.2.5. Superelasticity associating with martensite to martensite transformation below M_f. Figure 22 [26] shows typical stress-strain curves of the Au-47.5 at% Cd-0.25 at% Cu martensite phase alloy at room temperature just after the multiple interface transformation. Continuous yielding occurred at two stages, and the critical stress for the first plateau was extremely low (about 13.7 MPa) while that for the second plateau was high (107.6~137 MPa). When the applied stress was removed, the former left a residual strain but the latter did not. It is to be noticed that the second yielding is due to the formation of stress-induced martensite, i.e. martensite-to-martensite transformation. This residual strain was completely recovered on heating above the A_f temperature, indicating that the deformation did not occur by slip.

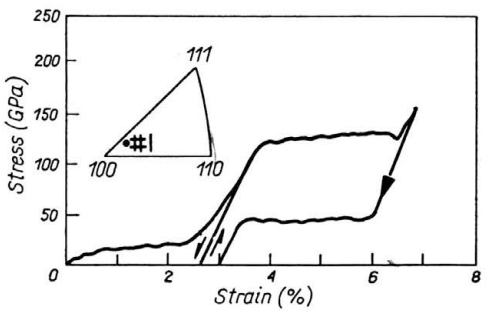

FIG. 22. Stress-strain curves obtained in the martensite specimen made by the multiple interface transformation.

Two-step yield points on the stress-strain curve are observed for Cu–Al–Ni by OTSUKA [27] and RODRIGUEZ and BROWN [28]. The stress-strain two step superelastic loop below M_f of a single crystal of Cu-14.0 wt% Al-4.2 wt% Ni with M_s = 306 K, M_f = 292 K, A_s = 301 K and A_f = 341 K is shown in Fig. 23. The first yield corresponds to γ_1' (thermal martensite) $\rightarrow \beta_1'$ transition and the second from $\beta_1' \rightarrow \alpha_1'$. The inverse transitions $\alpha_1' \rightarrow \beta_1' \rightarrow \gamma_1'$ take place on decreasing the stress. Laue patterns indicate that γ_1' is of AB' type (2H) and β_1' of $AB'CB'CA'CA'BA'$... type (18R) and α_1' of $AB'CA'CB'$ type (6R). OTSUKA *et al.* [29] assume phase relations between the parent phase β_1 and martensites

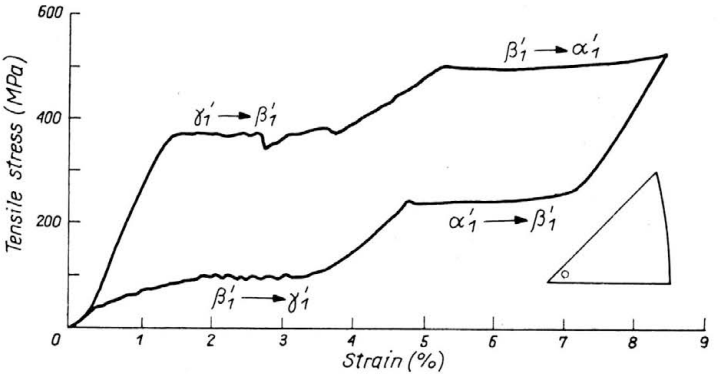

FIG. 23. Two-step yields associated with martensite to martensite transformations [27].

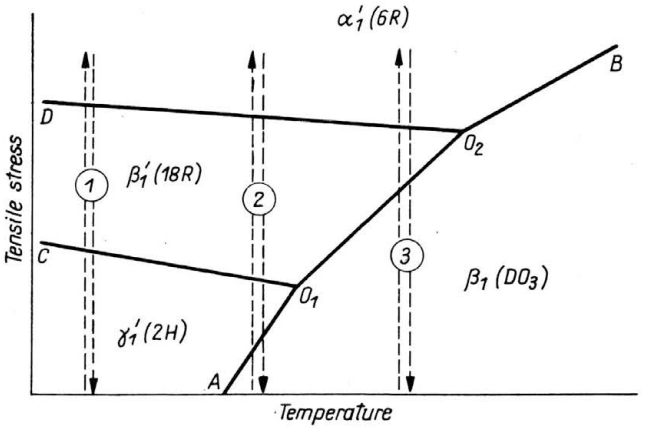

FIG. 24. Schematic phase relations between β_1 and γ_1', β_1' and α_1' as functions of stress and temperature.

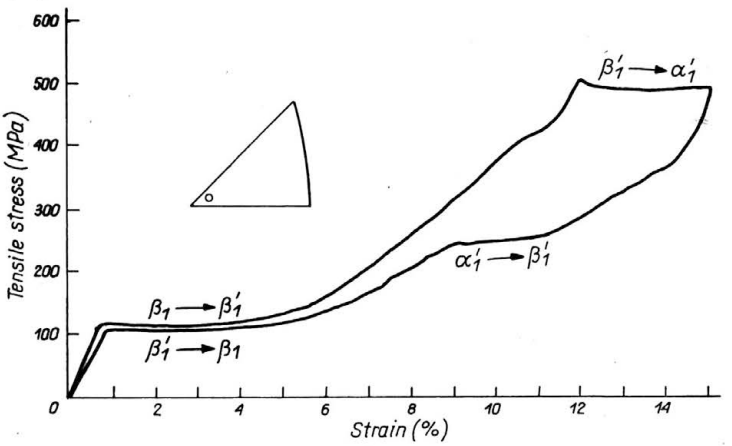

FIG. 25. A multistage superelastic stress-strain curve in the case ⟨3⟩.

γ_1', β_1' and α_1' as functions of stress and temperature as shown in Fig. 24. According to this phase diagram, several multistage superelasticities can be expected depending upon test temperatures. If the path ⟨1⟩ is taken in Fig. 24, the stress-strain behaviour as shown in Fig. 23 is obtained. If the path ⟨3⟩ is chosen, then the stress-strain curve of Fig. 25 is obtained. Although this is also a two-stage superelasticity, the nature and the shape of the curves are remarkably different from that of Fig. 23. In the former, the first stage superelasticity is due to the transformation between the matrix β_1 and martensite β_1' instead of the martensite-to-martensite transformation, the second stage being the same in the two cases.

Recently, OTSUKA *et al.* [8] have studied successive stress-induced martensite transformations in Cu–Al–Ni alloys, and their typical stress-strain curves as a function of temperature are shown in Fig. 26. These stress-strain curves may be divided into four temperature regimes according to the characteristics of the stress-strain curves: (I) $T < M_s$, (II) $M_s < T < A_f$, (III) $A_f < T < T_c$, (IV) $T_c < T$, where T_c is a certain critical temperature to be described later.

(I) $T < M_s$. This temperature range may be subdivided further into the two regions $T < M_f$ and $M_f < T < M_s$. In the former case, a specimen is brought into this temperature range by cooling in the absence of stress. Such a specimen consists of many variants of the γ_1' martensite initially, and it exhibits a three-stage yielding typically as shown in (b). The first stage represents the reorientation of the variants into a single crystal γ_1' martensite. At the second stage the nearly single crystal of the γ_1' martensite transforms into the β_1'' martensite. This β_1'' martensite was termed by MARTYNOV and KHANDROS [30] and its crystal structure and stacking sequence are shown in Table 2 and Fig. 5, respectively. At the third stage the β_1'' phase transforms into the α_1' one. The structure of this phase is essentially of the 6R type. The behaviour upon unloading from this stage is quite surprising. A recent study has shown clearly that the α_1' phase transforms not into β_1'' but into β_1' upon unloading. That is, the transformation upon unloading is not an exact reverse to that upon loading, but the strain attained upon loading almost completely recovers upon unloading. Similarly, the transformation from β_1' to γ_1' upon unloading is not an exact reverse to that at the second stage upon loading, but the strain attained upon loading at the second stage completely recovers upon unloading. The reason for this is simple. A macroscopic strain associated with the $\gamma_1' \rightarrow \beta_1''$ transformation is the same as that for the $\beta_1' \rightarrow \gamma_1'$ one. The same reasoning applies to the $\beta_1'' \rightarrow \alpha_1'$ and $\alpha_1' \rightarrow \beta_1'$ transformations. The product phase in the $\beta_1' \rightarrow \gamma_1'$ transformation upon unloading is a nearly single variant γ_1' martensite with $\{101\}\gamma_1'$ twins, which is stable at this temperature in the absence of stress. Thus the strain attained at the first stage does not recover at all. Next, if a complete single variant γ_1' martensite is loaded, the curve as shown in (b′) is obtained, which is quite similar to that in the second cycle in (b).

When a test temperature lies between M_f and M_s, a stress-strain curve of (c), which is similar to (b), is still obtained. The only difference is the first stage, where it now consists partly of the stress-induced transformation and partly of the reorientation of the γ_1' martensite, other general features being the same.

(II) $M_s < T < A_f$. The stress-strain curves in this temperature region exhibit three-stage yielding as typically shown in (d). They are similar to those in the region (I), except

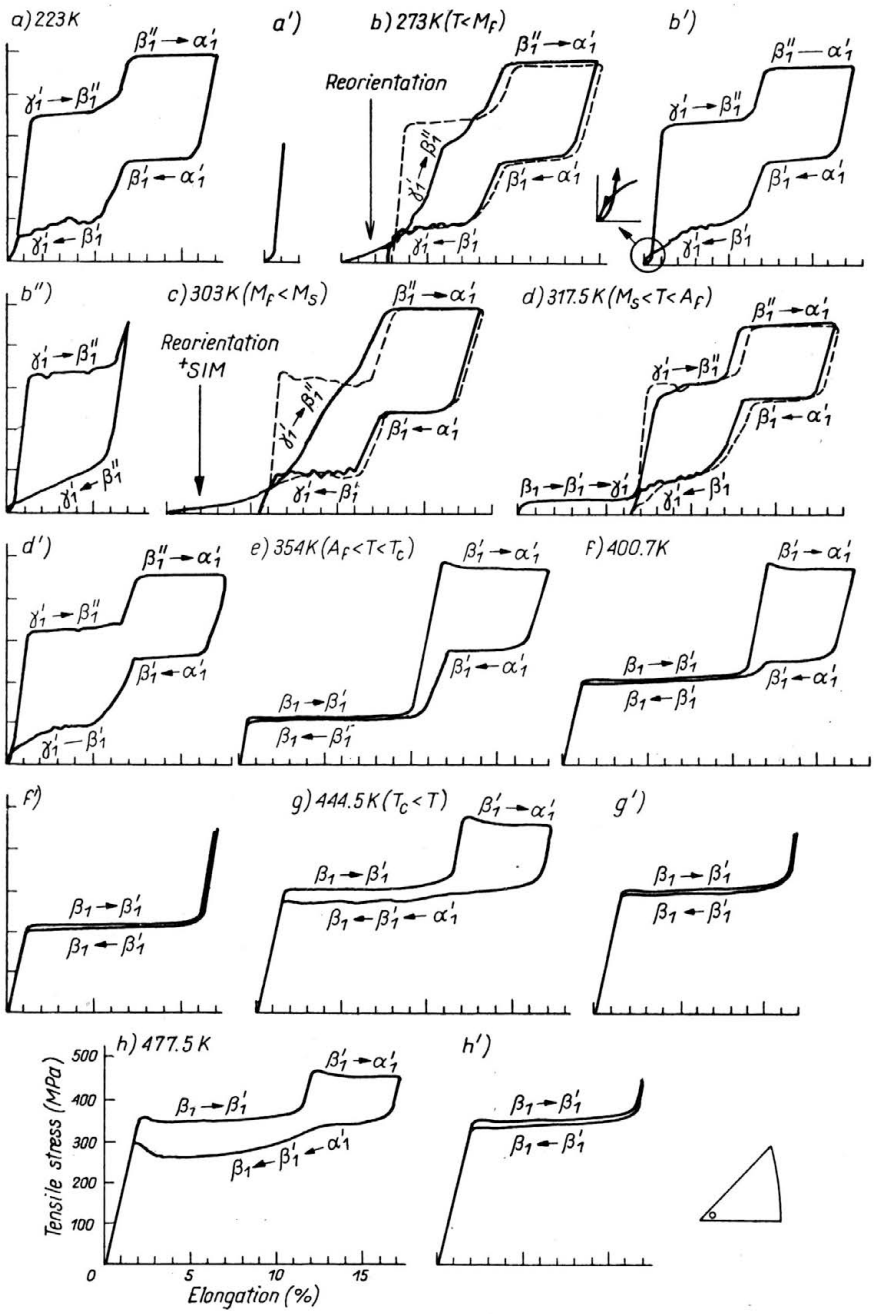

FIG. 26. Stress-strain curves as a function of temperature. Dotted lines in b), c) and d) represent the curves in the second cycle [8].

for the first stage. It now represents a stress-induced transformation rather than reorientation of the γ_1' martensite, since $T > M_s$. According to the phase diagram described later, it is expected that the γ_1' martensite is stress-induced in this temperature and stress region. But it is confirmed experimentally in the present alloy that the β_1' martensite is stress-induced and it subsequently transforms into the more stable γ_1' martensite at this stage. The reason for this is ascribed to the easiness of the nucleation of the β_1' martensite.

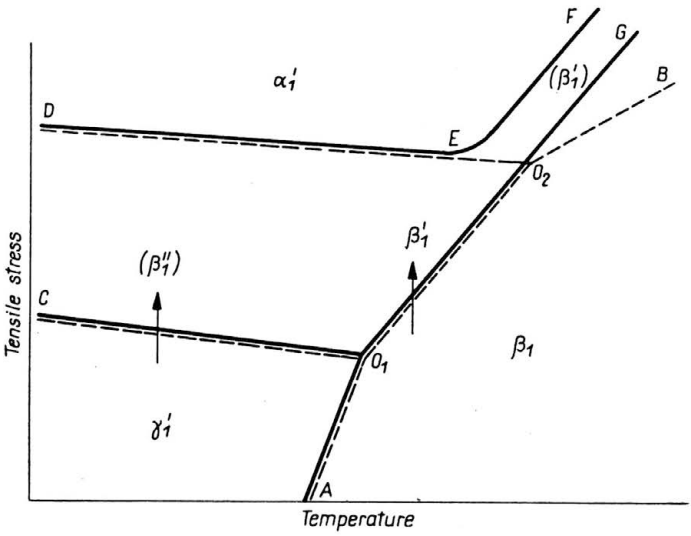

FIG. 27. Schematic stress-temperature phase diagram of a Cu–Al–Ni alloy. The diagram delineated by dashed lines is the one proposed previously [29], while that delineated by solid lines is the one deduced by the recent investigation [8].

compared to that of the γ_1' martensite. Since the resulting γ_1' martensite is stable in this temperature region, the strain attained at the first stage does not recover upon unloading. The behaviours of the second and third stages are essentially the same as before. Thus the well-defined stress-strain curve obtained from a single variant γ_1', (d), is also quite similar to those at lower temperatures [(b') and (a)].

(III) $A_f < T < T_c$. The stress-strain curves in this temperature region exhibit typical two-stage pseudoelasticity as shown in (e) and (f). The first stage is associated with a very small hysteresis, characteristic of the $\beta_1 \rightleftarrows \beta_1'$ transformation, while the latter with a large hysteresis. The critical stress for the $\beta_1 \rightarrow \beta_1'$ transformation increases with increasing temperature according to the Clausius-Clapeyron equation, while that for the $\beta_1' \rightarrow \alpha_1'$ transformation is rather temperature insensitive. Thus the stress gap between the critical stress for the $\alpha_1' \rightarrow \beta_1'$ transformation and that for the $\beta_1' \rightarrow \beta_1$ one decreases with increasing temperature defined as T_c. The curve of (f') shows that the linear portion between the first and second stages represents an elastic deformation of the β_1' martensite.

(IV) $T_c < T$. The stress-strain curve in this region exhibits two-stage yielding upon loading but only one-stage yielding upon unloading, as shown in (g), and the hysteresis at the first stage is much larger than those in the region (III).

Table 2. Crystal structures of the various stress-induced martensites in the present alloy.

Phase	γ_1'	β_1'	β_1''	α_1'
Space group	*P*nmm	*A* 2/m	*P* 2_1/m	*A* 2/m
Lattice parameter				
a (nm)	0.4382	~0.44	0.4437	
b	0.5356	~0.53	0.5301	
c	0.4222	~3.80	3.814	
β		~90°	89.24°	
Ramsdel notation	2*H*	$18R_1$	$18R_2$	6R
Zhdanov symbol	$1\bar{1}$	$(2\bar{1})_6$	$(1\bar{1}3\bar{1})_3$	$(1)_6$
Stacking sequence	*AB'*	*AB'CB'CA'* *CA'BA'BC'* *BC'AC'AB'*	*AB'AB'CA'* *CA'CA'BC'* *BC'BC'AB'*	*AB'CA'BC'*

Otsuka *et al.* deduced a phase diagram where an equilibrium point was determined by taking a mid-point of the two critical stresses for the forward and reverse transformations and this diagram, as shown in Fig. 27, has three complexities which must be compared with that already shown in Fig. 24.

One is the phase field O_1CDO_2. At first sight, based on the phase rule, it looks like a single-phase field of β_1', but the fact that β_1'' is stress-induced from γ_1' contradicts this statement. This contradiction may be rationalized by a more recent work by SHIMIZU *et al.* [31]. They indicated from the back-reflection Laue photography under tension that β_1'' is simply a metastable phase, and that the real stable phase in this phase field is β_1'. The reason for the appearance of the β_1'' martensite can be explained by considering the transformation mechanism.

Another complexity is the high temperature region. In Fig. 24 Otsuka *et al.* predicted the presence of the triple point O_2 or the direct transformation from β_1 to α_1', but this prediction was not observed in this investigation. The stress-strain curves in Fig. 26 have shown that the β_1 matrix phase always transforms to the α_1' phase *via* the β_1' phase. The third complexity is the region including the line AO_1. We expect direct transformation from β_1 to γ_1' in this region. However, direct transformation was not detected in the present alloy, as already shown in Fig. 26d. If the line AO_1 is short, the nucleation of β_1' is favoured even though γ_1' is more stable thermodynamically.

References

1. J. W. CHRISTIAN, *The theory of transformations in metals and alloys*, Pergamon Press, Oxford 1965.
2. L. DELAEY, P. F. GOLBIN, G. GUENIN and H. WARLIMONT, Proc. of Int. Conf. of Martensitic Transformations, ICOMAT-79, Cambridge, Mass., 400, 1979.
3. H. SUZUKI, *Physical properties of metals*, [in Japanese], Shokabo, Tokyo, 394, 1968.
4. E. E. LAHTEENKORVA, Annales Academiae Scientiarum Fennicae, Ser. A. VI, Physica, 87, 1961.
5. K. SHIMIZU and K. OTSUKA, *Shape memory effects in alloys*, Plenum Press, New York, 59, 1975.
6. Z. S. BASINSKI and J. W. CHRISTIAN, Acta Met., **2**, 101, 1954.
7. C. M. WAYMAN and K. SHIMIZU, Metal Sci. J., **6**, 175, 1972.

8. K. OTSUKA, H. SAKAMOTO and K. SHIMIZU, Acta Met., **27**, 585. 1979.
9. Z. NISHIYAMA, *Martensitic transformations*, Academic Press, London, 1978.
10. T. TADAKI, Thesis, Osaka University, 113, 1978.
11. Z. NISHIYAMA and K. KAJIWARA, Jap. J. Appl. Phys., **2**, 478. 1963.
12. (a) K. OTSUKA and C. M. WAYMAN, *Reviews on the deformation behavior of metals*, Freund Publishing House, Israel, 81, 1977. (b) N. NAKANISHI, *New aspects of martensitic transformation*, Supp. Trans. J. Inst. Metals, **17**, 211, 1976. (c) K. OISHI and L. C. BROWN, Metall. Trans., **2**, 1971, 1971. (d) N. NAKANISHI, T. MORI, S. MIURA, Y. MURAKAMI and S. KACHI, Phil. Mag., **28**, 277, 1973.
13. K. AIZU, J. Phys. Soc. Japan, **27**, 387, 1969.
14. K. HAZAMA, Plastics, **24**, 33, 1974.
15. J. Y. GUEDOU, M. PALIARD and J. RIEU, Scripta Met., **10**, 631, 1976.
16. S. MIURA, T. MORI, N. NAKANISHI, Y. MURAKAMI and S. KACHI, Phil. Mag., **34**, 337, 1976.
17. L. C. L. CHANG and T. A. READ, Trans. AIME, **189**, 47, 1951.
18. N. NAKANISHI, Y. MURAKAMI, S. KACHI, T. MORI and S. MIURA, Phys. Lett., A **37**, 61, 1971.
19. H. WARLIMONT and L. DELAEY, Progress in Materials Science, Pergamon Press, Oxford, **18**, 1974.
20. L. DELAEY, F. V. VOORDE and R. V. KRISHNAN, *Shape memory effects in alloys*, Plenum Press, New York, 351, 1975.
21. T. SABURI and C. M. WAYMAN, Acta Met., **28**, 1, 1980.
22. H. M. LEDBETTER and C. M. WAYMAN, Met. Trans., **3**, 2349, 1972.
23. H. K. BIRNBAUM and T. A. READ, Trans. AIME, **218**, 662, 1960.
24. S. MIURA, S. MAEDA and N. NAKANISKI, Phil. Mag., **30**, 565, 1974.
25. D. S. LIEBERMAN, M. A. SCHMERLING and R. W. KARZ, *Shape memory effects in alloys*, Plenum Press, New York, 203, 1975.
26. S. MIURA, M. ITO, F. HORI and N. NAKANISHI, *New aspects of martensitic transformation*, Supp. Trans. J. Inst. Metals, **17**, 257, 1976.
27. K. OTSUKA, H. SAKAMOTO and K. SHIMIZU, Scripta Met., **10**, 983, 1976.
28. C. RODRIGUEZ and L. C. BROWN, Metall. Trans., **7A**, 265, 1976.
29. K. OTSUKA, C. M. WAYMAN, K. NAKAI, H. SAKAMOTO and K. SHIMIZU, Acta Met., **24**, 207, 1976.
30. V. V. MARTYNOV and L. G. KHANDROS, Int. Conf. on Martensitic Transformation, Kiev, May, 123, 1977.
31. K. SHIMIZU, H. SAKAMOTO and K. OTSUKA, Scripta Met., **12**, 771, 1978.

DEPARTMENT OF CHEMISTRY, FACULTY OF SCIENCE
KONAN UNIVERSITY, KOBE, JAPAN.

Received September 18, 1981.